Letters in Applied Microbiology. 65 (5): 446-452 (2018).

The final publication is available at https://onlinelibrary.wiley.com/doi/abs/10.1111/lam.12797

Increased metabolite production by deletion of an HDA1-type histone deacetylase in the phytopathogenic fungi, *Magnaporthe oryzae* (*Pyricularia oryzae*) and *Fusarium asiaticum*

K. Maeda[1,2,3,†], M. Izawa[1,4,†], Y. Nakajima[2,†], Q. Jin[2], T. Hirose[1,3], T. Nakamura[5], H. Koshino[5], K. Kanamaru[2], S. Ohsato[3], T. Kamakura[4] , T. Kobayashi[2], M. Yoshida[1] and M. Kimura[1,2]

[1] Chemical Genetics Laboratory, RIKEN, 2-1 Hirosawa, Wako, Saitama 351-0198, Japan

[2] Department of Biological Mechanisms and Function, Graduate School of Bioagricultural Sciences, Nagoya University, Furo-cho, Chikusa-ku, Nagoya, Aichi 464-8601, Japan

[3] Graduate School of Agriculture, Meiji University, 1-1-1 Higashi-Mita, Tama-ku, Kawasaki, Kanagawa 214-8571, Japan

[4] Faculty of Science and Technology, Tokyo University of Science, 2461 Yamazaki, Noda, Chiba 278-8510, Japan

[5] Molecular Structure Characterization Unit, RIKEN Center for Sustainable Resource Science (CSRS), 2-1 Hirosawa, Wako, Saitama 351-0198, Japan

Running head: HDAC regulation of natural products

[†] Joint first authors

Correspondence

Makoto Kimura, Department of Biological Mechanisms and Function, Graduate School of Bioagricultural Sciences, Nagoya University, Furo-cho, Chikusa-ku, Nagoya, Aichi 464-8601, Japan

E-mail: mkimura@agr.nagoya-u.ac.jp

Significance and Impact of the Study: Natural products of fungi have significant impacts on human welfare, in both detrimental and beneficial ways. Although HDA1-type histone deacetylase is not essential for vegetative growth, deletion of the gene affects the expression of clustered secondary metabolite genes in some fungi. Here, we report that such phenomena are also observed in physically unlinked genes required for melanin biosynthesis in the rice blast fungus. In addition, production of *Fusarium* trichothecenes, previously reported to be unaffected by HDA1 deletion, was significantly upregulated in another *Fusarium* species. Thus, the HDA1-inactivation strategy may be regarded as a general approach for overproduction and/or discovery of fungal metabolites.

Abstract

Histone deacetylases (HDACs) play an important role in the regulation of chromatin structure and gene expression. We found that dark pigmentation of *Magnaporthe oryzae* (anamorph *Pyricularia oryzae*) Δ*Mohda1*, a mutant strain in which an ortholog of the yeast *HDA1* was disrupted by double cross-over homologous recombination, was significantly stimulated in liquid culture. Analysis of metabolites in a Δ*Mohda1* mutant culture revealed that the accumulation of shunt products of the 1,8-dihydroxynaphthalene melanin and ergosterol pathways were significantly enhanced compared to the wild-type strain. Northern blot analysis of the Δ*Mohda1* mutant revealed transcriptional activation of three melanin genes that are dispersed throughout the genome of *M. oryzae*. The effect of deletion of the yeast *HDA1* ortholog was also observed in *Fusarium asiaticum* from the *Fusarium graminearum* species complex; the *HDF2* deletion mutant produced increased levels of nivalenol-type trichothecenes. These results suggest that histone modification via HDA1-type HDAC regulates the production of natural products in filamentous fungi.

Keywords: biosynthesis gene cluster; fungal natural products; histone acetylation/deacetylation; rice blast fungus; wheat scab fungus

Introduction

Histone deacetylases (HDACs) play an important role in eukaryotic transcriptional regulation by reducing the acetylation status of histones, which is necessary for chromatin modifications and nucleosome assembly (Steinfeld *et al.* 2007). In *Aspergillus* species, HDACs can be classified into two major groups based on the sequence similarities with those of *Saccharomyces cerevisiae*: (i) two classes of classical HDACs, RPD3-type (class 1) comprised of RpdA and HosA, and HDA1-type (class 2) comprised of HdaA (yeast Hda1p), and fungal-specific HosB that is more distantly related to both of these classes (classified either as class 2 or as a third group between these classes) (Lamoth *et al.* 2015), and (ii) NAD^+-dependent SIR2-type enzyme HstA, also referred to as class 3. In the model filamentous fungus *Aspergillus nidulans*, trichostatin A (TSA)-sensitive HdaA represents the major HDAC activity in the mycelia and contributes to normal growth under oxidative stress conditions (Tribus *et al.* 2005). However, RpdA, but not HdaA, is critical for growth, as shown by the fact that genetic depletion of *AnRpdA* by gene knockdown results in a pronounced reduction in growth and sporulation (Tribus *et al.* 2010).

Secondary metabolites of filamentous fungi are a potentially rich source of bioactive small molecules that can be used for medical and pharmaceutical purposes. Most secondary metabolite genes are clustered, which is thought to be important for coregulation of the clustered genes via modification of the associated chromatin structure (Chiou *et al.* 2002). To assess possible epigenetic histone modifications, the contribution of HDACs to secondary metabolism was investigated in *A. nidulans*. As anticipated, the telomere-proximal gene clusters of mycotoxin sterigmatocystin and antibiotic penicillin were specifically upregulated in the *AnhdaA* deletion strain (Shwab *et al.* 2007). From these studies, HdaA was proposed to be involved in the negative regulation of subtelomeric secondary metabolite gene cluster. In *A. fumigatus*, however,

deletion of *AfhdaA* did not affect growth under oxidative stress conditions and resulted in both positive and negative regulation of secondary metabolite genes (Lee *et al.* 2009). Moreover, there was no correlation between distance from the telomere and HdaA-mediated regulation of secondary metabolite genes. In *Fusarium fujikuroi*, deletion of an *hdaA* ortholog, *Ffhda1*, not only altered the amount of secondary metabolites such as gibberellic acids, fusaric acid, and bikaverin, but also abrogated the regulation of bikaverin biosynthesis (Studt *et al.* 2013). Taken together, these data suggest that an HDA1-type HDAC can modulate the expression of secondary metabolite cluster genes, either positively or negatively, in filamentous fungi.

In our molecular genetic studies on growth and differentiation of the plant pathogenic fungus *Magnaporthe oryzae* (anamorph *Pyricularia oryzae*), we found that dark pigmentation was somewhat increased in Δ*Mohda1* mutants, which lack the HDA1-type enzyme MoHDA1 (Izawa *et al.* 2009). Other HDAC mutants, including Δ*Mohos2* and Δ*Mohos3*, did not show such significant differences in pigmentation compared to wild-type. The enhanced dark pigmentation appeared to be caused by activation of polyketide metabolism of the 1,8-dihydroxynaphthalene (DHN) melanin pathway. This metabolic pathway activation is similar to a case where sterigmatocystin and penicillin production was increased by the Δ*AnhdaA* mutant of *A. nidulans* (Shwab *et al.* 2007), in which HdaA contributes to repression of the corresponding cluster gene expression during early fungal growth. However, distinct from the de-repression of these secondary metabolite cluster genes, melanin biosynthetic genes are dispersed throughout the genome of *M. oryzae* in three different loci.

In the current study, we examined the effect of deletion of an HDA1-type HDAC on the biosynthesis of natural products in *M. oryzae*. The regulatory role of histone modification was also studied using *Fusarium asiaticum* (*Fusarium graminearum* species complex), another important model cereal pathogen more closely related to *M. oryzae* than *Aspergillus* species.

Results and discussion

Identification of the metabolites that are increased in the Δ*Mohda1* mutant

To gain some insight into the molecular mechanisms that underlie the increased dark pigmentation observed in the Δ*Mohda1* mutant (Fig. 1A), we sought to define the time course of metabolite accumulation in a YGPCa culture. The metabolites extracted from culture supernatant (5 ml) at different time points (24, 48, and 72 h after transfer to the medium) were analyzed by thin layer chromatography (TLC). When visualized by fluorescence at an excitation wavelength of 312 nm, four metabolites (**1**, **2**, **3**, and **4** at R_f value of 0.38, 0.45, 0.64, and 0.89, respectively; **1**, **2**, and **3** could also be detected by UV absorption at 254 nm) were found to be significantly increased in Δ*Mohda1* mutant cultures compared to wild-type (Fig. 1B).

Analysis of purified **1** − **3** with ^{1}H-NMR and ^{13}C-NMR identified them as known shunt metabolites of the DHN melanin biosynthesis pathway (Fig. S1A): 3,4,8-trihydroxytetralone (3,4,8-THT, **1**) (Iwasaki *et al.* 1973), 4,6,8-trihydroxytetralone (4,6,8-THT, **2**) (Iwasaki *et al.* 1973), and 4,8-dihydroxytetralone (4,8-DHT, **3**) (Morita and Aoki 1974) (Fig. 1C and Fig. S2). EI-MS spectrum of purified **4** matched to that of ergosta-4,6,8(14),22-tetraen-3-one (ergone) (White and Taylor 1970) (Fig. 1C and Fig. S3), a shunt product derived from ergosterol by peroxidation, peroxide cleavage, and dehydrations (Fig. S1B).

Melanin biosynthesis involves enzymes encoded by genes that are not clustered at a single locus, as opposed to clustered secondary metabolite genes that are regulated by chromatin modification. Enhanced production of these natural metabolites suggests that their biosynthesis can also be regulated by inactivation of HDA1-type HDAC activity, without significant growth defect. Indeed, addition of TSA (1 μg ml^{-1} = 3.3 μM)

resulted in enhanced levels of melanization and an accumulation of shunt metabolites (**1** – **4**) (Fig. S4). These results indicate that HDAC inhibition deserves to be tested for use in overproduction and/or discovery of fungal metabolites as previously proposed (Shwab *et al.* 2007), including those whose biosynthesis is dependent on the genes dispersed in the fungal genome.

Analysis of DHN melanin gene expression and histone modifications in *M. oryzae*

Fungal melanin is formed by oxidative polymerization of DHN, in which a laccase has been hypothesized to play a central role. The first intermediate of the DHN melanin pathway, 1,3,6,8-tetrahydroxynaphthalene (T4HN), undergoes two rounds of alternate reduction and dehydration (Fig. S1A), then the pathway proceeds *via* scytalone, 1,3,8-trihydroxynaphthalene (T3HN), and vermelone to DHN. All of the known DHN melanin biosynthesis genes are located at non-subtelomeric regions. The T3HN reductase gene [*BUF1*; MGG_02252] is 1.2 Mb from the chromosome 1 telomere, scytalone dehydratase gene [*RSY1*; MGG_05059] is 2.2 Mb from the chromosome 3 telomere, and T4HN reductase [*4HNR*; MGG_07216], polyketide synthase [*ALB1*; MGG_07219], and putative melanin genes are clustered at a locus 1.5 Mb from the chromosome 2 telomere. To gain insight into the mechanism that underlies increased production of the shunt metabolites (**1** – **3**), we analyzed the expression of three representative melanin genes on different chromosomes.

After sampling the supernatant for metabolites at each time point, we isolated total RNA from the mycelia and performed northern blot analysis (Fig. 1D). The Δ*Mohda1* mutant showed upregulated expression of physically unlinked melanin genes, *4HNR*, *RSY1*, and *BUF1*, at 48 h, when the spot intensities of the melanin shunt metabolites obviously exceeded those of the wild-type strain. In wild-type, transcript levels of the melanin genes, except *4HNR*, increased to levels comparable to those of the Δ*Mohda1* mutant after 72 h of incubation. Thus, this stimulation of shunt product

accumulation is likely to be due to the overall differences in gene expression between the wild-type and mutant prior to the 72 h time point.

The degree of histone H3 general (H3) and lysine 9 (H3K9) acetylations (H3Ac and H3K9Ac), H3K9 trimethylation (H3K9me3), and histone H4 general (H4) acetylation (H4Ac) did not differ significantly throughout the incubation period after deletion of *Mohda1* (Fig. S5). Thus, similar to the *Aspergillus* species (Palmer *et al.* 2008; Lee *et al.* 2009), other HDACs may play complementary roles to keep the overall histone modification level unaffected in *M. oryzae*.

Generally, lysines of H3 and H4 are acetylated in transcriptionally active chromatin. Chromatin immunoprecipitation (ChIP) with anti-acetyl histone antibodies demonstrated acetylations of H3 and H4 that are positioned at transcriptionally active promoters of sterigmatocystin and aflatoxin biosynthesis genes (Roze *et al.* 2007; Reyes-Dominguez *et al.* 2010). Concomitant with increasing levels of acetylated H3, the level of H3K9me3, which is correlated with heterochromatin formation, decreases in the promoters of activated genes (Reyes-Dominguez *et al.* 2010). Thus, histones positioned at the three actively transcribed melanin gene loci may also be locally hyperacetylated under the melanin-producing conditions. ChIP with high-throughput sequencing may provide some clues about the altered expression of the three physically unlinked natural product genes following deletion of *Mohda1*.

Trichothecene productivity in *HDF2* deletion mutants of the *F. graminearum* species complex

Next, we disrupted *HDF2* (Li *et al.* 2011), the HDA1-type HDAC gene of *F. asiaticum,* to examine its contribution to trichothecene biosynthesis. The entire coding region of *F. asiaticum HDF2* was deleted via double cross-over homologous recombination (Fig. S6A). Deletion of *HDF2* was confirmed in three independent transformants (Tr6, Tr16, and Tr18) by PCR (Fig. S6B) and Southern blot analysis (Fig. S6C), which

demonstrated targeted integration of the gene disruption vector into their genome.

By using the Δ*hdf2* deletion mutants, we compared the time course of trichothecene accumulation to that of the wild-type strain. The three independent transformants were cultured in boiled rice flour liquid medium and the amount of trichothecene in each was determined after 7 and 14 days of incubation. As shown in Fig. 2A, accumulation of the nivalenol (NIV)-type trichothecenes by the mutants had exceeded that of the wild-type. The stimulation of NIV-type trichothecene production was supported statistically by the results of triplicate experiments, indicating that the regulation of trichothecene biosynthesis was altered by deletion of *HDF2*.

In the genome of *F. graminearum* species complex, most of the trichothecene biosynthesis genes (*Tri* genes) are clustered (Kimura *et al.* 2007). *Tri6*, encoding a trichothecene pathway-specific transcription factor, positively regulates expression of other *Tri* genes, including *Tri5* responsible for the first biosynthetic step. The expression of these *Tri* genes was analyzed by northern blot analysis using one of the deletion mutants, Δ*hdf2*-Tr6. At day 3, expression level of *Tri5* was significantly higher in the mutant compared to the wild-type, when cultured in YS_60 medium (Fig. 2B). Accumulation of *Tri6* mRNA was also higher, but the peak appeared to have occurred at an earlier time point. At days 5 and 7, expression levels of these *Tri* genes were slightly higher in the mutant compared to the wild-type. These results suggest that stimulation of trichothecene accumulation is due to transcriptional activation of *Tri* genes by deleting *HDF2*.

In a previous study, deletion of *HDF2* of *F. graminearum* strain PH-1 did not significantly affect production of trichothecenes (Li *et al.* 2011). While strain MAFF 111233 belongs to lineage 6 in the *F. graminearum* species complex, strain PH-1 belongs to lineage 7, *F. graminearum sensu stricto*. Thus, we used the same lineage 7, *F. graminearum* strain JCM 9873, to determine whether trichothecene production was affected by the same mutation. *HDF2* was deleted and trichothecene productivity was

compared to that of the wild-type. TLC analysis of the culture extracts showed spots of 15-acetyldeoxynivalenol (15-ADON) with similar color intensity, suggesting that trichothecene productivity was not altered by the mutation (Fig. S7). These results indicate that even closely-related strains are differentially affected by the deletion of HDA1-type HDAC. Thus, if the HDA1-inactivation strategy for increased secondary metabolite production does not work for one fungal strain, the effect should still be tested in other closely related strains.

Materials and methods

Strains and media

The Δ*Mohda1* mutant strain H1D15 and its parent strain P2 of *M. oryzae* were used to compare metabolite profiles (Izawa *et al.* 2009). *F. asiaticum* strain MAFF 111233 and *F. graminearum* strain JCM 9873 were used as trichothecene producers. MAFF 111233 produces nivalenol (NIV)-type trichothecenes 4,15-diacetylnivalenol (4,15-diANIV) and 4-acetylnivalenol (4-ANIV) and JCM 9873 produces 15-ADON in liquid culture.

Young mycelia of *M. oryzae* were transferred to melanin-inducing YGPCa medium (0.5% yeast extract, 2% glucose, 0.05% $Na_2HPO_4 \cdot 12H_2O$, 0.05% KH_2PO_4, 0.001% $CaCl_2$) and incubated at 28°C in the dark with reciprocal shaking (120 strokes min^{-1}). *Fusarium* strains were maintained on V8 agar medium (Maeda *et al.* 2016) with or without 300 μg ml^{-1} hygromycin B. To induce trichothecene production, strain MAFF 111233 was incubated at 22°C in the boiled rice flour liquid medium (Maeda *et al.* 2016) or YS_60 medium (Nakajima *et al.* 2014) with gyratory shaking (160 rpm).

Chemical analysis

The culture supernatants of *M. oryzae* and the *F. graminearum* species complex were

extracted with equal amount of ethyl acetate and the solvent was evaporated under nitrogen. The dried samples were then dissolved in small amounts of methanol and separated on TLC plates (silica gel 60 F_{254}, Merck Millipore, Darmstadt, Germany) using ethyl acetate/toluene (3:1) as the solvent. For purification of *M. oryzae* metabolites, major spots on the TLC plates were visualized by fluorescence, the relevant areas in the silica gel layer were scraped off, and compounds were eluted with ethyl acetate. Compounds **1**–**3** were further purified by HPLC equipped with a PEGASIL ODS SP100 column (6.0 φ × 250 mm; Senshu Scientific Co., Tokyo) by isocratic elution with 20% acetonitrile. Compound **4** was purified using a PEGASIL C4 SP100 column (6.0 φ × 250 mm; Senshu Scientific) with 70% acetonitrile. EI mass and NMR spectra were obtained using a JMS-SX102A and JMS-HX110 mass spectrometers (JEOL Ltd., Akishima, Japan) and JNM-ECA600 (JEOL) spectrometer, respectively. 4,15-diANIV and 4-ANIV were visualized by TLC or quantified by HPLC as previously described (Ochiai *et al.* 2007).

Molecular biology and biochemical analysis of *M. oryzae*

For northern blot analysis of melanin genes, total RNA (10 μg) was blotted onto a Nytran N nylon membrane (GE Healthcare Japan Co., Tokyo) and hybridized with the digoxigenin (DIG)-labeled DNA probes, which were prepared using a PCR-DIG Probe Synthesis kit (Roche Diagnostics K.K., Tokyo) (see Table S1 for the primers). RNA-DNA probe hybrid was generated in DIG Easy Hyb (Roche) hybridization solution at 50°C, washed according to the manufacturer's instructions, and detected using a DIG Luminescent Detection kit (Roche).

Molecular genetic analysis of the *F. graminearum* species complex

For targeted gene deletion of *HDF2* (Li *et al.* 2011), the HDA1-type HDAC gene of *F. graminearum* species complex, a gene disruption vector pΔFgHda1 was constructed.

Primers were synthesized for amplification of homologous regions, based on the genome sequence database for *F. graminearum* PH-1 (Table S1), and used to construct pΔFgHda1 by the inverse PCR (IPCR) method (Banno *et al.* 2003). pΔFgHda1 was linearized with *Not*I and transformed into *F. asiaticum* MAFF 111233 and *F. graminearum* JCM 9873, as previously described (Tokai *et al.* 2007).

Genomic DNA was isolated from hygromycin B-resistant colonies and used to screen for Δ*hdf2* deletion mutants by PCR using primers listed in Table S1. Targeted integration of the vector was confirmed by Southern blotting with DIG-labeled DNA probes (see Table S1 for primers). Northern blot analysis of *Tri6* and *Tri5* was done as described for *M. oryzae* (see Table S1 for the primers).

Acknowledgements

This research was partially supported by the Tojuro Iijima Foundation for Food Science and Technology.

Conflict of interest

The authors declare no conflict of interest.

References

Banno, S., Kimura, M., Tokai, T., Kasahara, S., Higa-Nishiyama, A., Takahashi-Ando, N., Hamamoto, H., Fujimura, M., Staskawicz, B.J. and Yamaguchi, I. (2003) Cloning and characterization of genes specifically expressed during infection stages in the rice blast fungus. *FEMS Microbiol Lett* **222**, 221-227.

Chiou, C.H., Miller, M., Wilson, D.L., Trail, F. and Linz, J.E. (2002) Chromosomal location plays a role in regulation of aflatoxin gene expression in *Aspergillus parasiticus*. *Appl Environ Microbiol* **68**, 306-315.

Iwasaki, S., Muro, H., Sasaki, K., Nozoe, S., Okuda, S. and Sato, Z. (1973) Isolations of phytotoxic substances produced by *Pyricularia oryzae* Cavara. *Tetrahedron Lett*, 3537-3542.

Izawa, M., Takekawa, O., Arie, T., Teraoka, T., Yoshida, M., Kimura, M. and Kamakura, T. (2009) Inhibition of histone deacetylase causes reduction of appressorium formation in the rice blast fungus *Magnaporthe oryzae*. *J Gen Appl Microbiol* **55**, 489-498.

Kimura, M., Tokai, T., Takahashi-Ando, N., Ohsato, S. and Fujimura, M. (2007) Molecular and genetic studies of *Fusarium* trichothecene biosynthesis: pathways, genes, and evolution. *Biosci Biotechnol Biochem* **71**, 2105-2123.

Lamoth, F., Juvvadi, P.R. and Steinbach, W.J. (2015) Histone deacetylase inhibition as an alternative strategy against invasive aspergillosis. *Front Microbiol* **6**, 96.

Lee, I., Oh, J.H., Shwab, E.K., Dagenais, T.R., Andes, D. and Keller, N.P. (2009) HdaA, a class 2 histone deacetylase of *Aspergillus fumigatus*, affects germination and secondary metabolite production. *Fungal Genet Biol* **46**, 782-790.

Li, Y., Wang, C., Liu, W., Wang, G., Kang, Z., Kistler, H.C. and Xu, J.R. (2011) The *HDF1* histone deacetylase gene is important for conidiation, sexual reproduction, and pathogenesis in *Fusarium graminearum*. *Mol Plant Microbe Interact* **24**,

487-496.

Maeda, K., Tanaka, A., Sugiura, R., Koshino, H., Tokai, T., Sato, M., Nakajima, Y., Tanahashi, Y., Kanamaru, K., Kobayashi, T., Nishiuchi, T., Fujimura, M., Takahashi-Ando, N. and Kimura, M. (2016) Hydroxylations of trichothecene rings in the biosynthesis of *Fusarium* trichothecenes: evolution of alternative pathways in the nivalenol chemotype. *Environ Microbiol* **18**, 3798-3811.

Morita, T. and Aoki, H. (1974) Isosclerone, a new metabolite of *Sclerotinia sclerotiorum* (LIB.) DE BARY. *Agric Biol Chem* **38**, 1501-1505.

Nakajima, Y., Tokai, T., Maeda, K., Tanaka, A., Takahashi-Ando, N., Kanamaru, K., Kobayashi, T. and Kimura, M. (2014) A set of heterologous promoters useful for investigating gene functions in *Fusarium graminearum*. *JSM Mycotoxins* **64**, 147-152.

Ochiai, N., Tokai, T., Takahashi-Ando, N., Fujimura, M. and Kimura, M. (2007) Genetically engineered *Fusarium* as a tool to evaluate the effects of environmental factors on initiation of trichothecene biosynthesis. *FEMS Microbiol Lett* **275**, 53-61.

Palmer, J.M., Perrin, R.M., Dagenais, T.R. and Keller, N.P. (2008) H3K9 methylation regulates growth and development in *Aspergillus fumigatus*. *Eukaryot Cell* **7**, 2052-2060.

Reyes-Dominguez, Y., Bok, J.W., Berger, H., Shwab, E.K., Basheer, A., Gallmetzer, A., Scazzocchio, C., Keller, N. and Strauss, J. (2010) Heterochromatic marks are associated with the repression of secondary metabolism clusters in *Aspergillus nidulans*. *Mol Microbiol* **76**, 1376-1386.

Roze, L.V., Arthur, A.E., Hong, S.-Y., Chanda, A. and Linz, J.E. (2007) The initiation and pattern of spread of histone H4 acetylation parallel the order of transcriptional activation of genes in the aflatoxin cluster. *Mol Microbiol* **66**, 713-726.

Shwab, E.K., Bok, J.W., Tribus, M., Galehr, J., Graessle, S. and Keller, N.P. (2007) Histone deacetylase activity regulates chemical diversity in *Aspergillus*. *Eukaryot Cell* **6**, 1656-1664.

Steinfeld, I., Shamir, R. and Kupiec, M. (2007) A genome-wide analysis in *Saccharomyces cerevisiae* demonstrates the influence of chromatin modifiers on transcription. *Nat Genet* **39**, 303-309.

Studt, L., Schmidt, F.J., Jahn, L., Sieber, C.M., Connolly, L.R., Niehaus, E.M., Freitag, M., Humpf, H.U. and Tudzynski, B. (2013) Two histone deacetylases, *FfHda1* and *FfHda2*, are important for *Fusarium fujikuroi* secondary metabolism and virulence. *Appl Environ Microbiol* **79**, 7719-7734.

Tokai, T., Koshino, H., Takahashi-Ando, N., Sato, M., Fujimura, M. and Kimura, M. (2007) *Fusarium Tri4* encodes a key multifunctional cytochrome P450 monooxygenase for four consecutive oxygenation steps in trichothecene biosynthesis. *Biochem Biophys Res Commun* **353**, 412-417.

Tribus, M., Bauer, I., Galehr, J., Rieser, G., Trojer, P., Brosch, G., Loidl, P., Haas, H. and Graessle, S. (2010) A novel motif in fungal class 1 histone deacetylases is essential for growth and development of *Aspergillus*. *Mol Biol Cell* **21**, 345-353.

Tribus, M., Galehr, J., Trojer, P., Brosch, G., Loidl, P., Marx, F., Haas, H. and Graessle, S. (2005) HdaA, a major class 2 histone deacetylase of *Aspergillus nidulans*, affects growth under conditions of oxidative stress. *Eukaryot Cell* **4**, 1736-1745.

White, J.D. and Taylor, S.I. (1970) Biosynthesis of ergosta-4,6,8(14),22-tetraen-3-one. *In vivo* incorporation of a 1,4-dioxide. *J Am Chem Soc* **92**, 5811-5813.

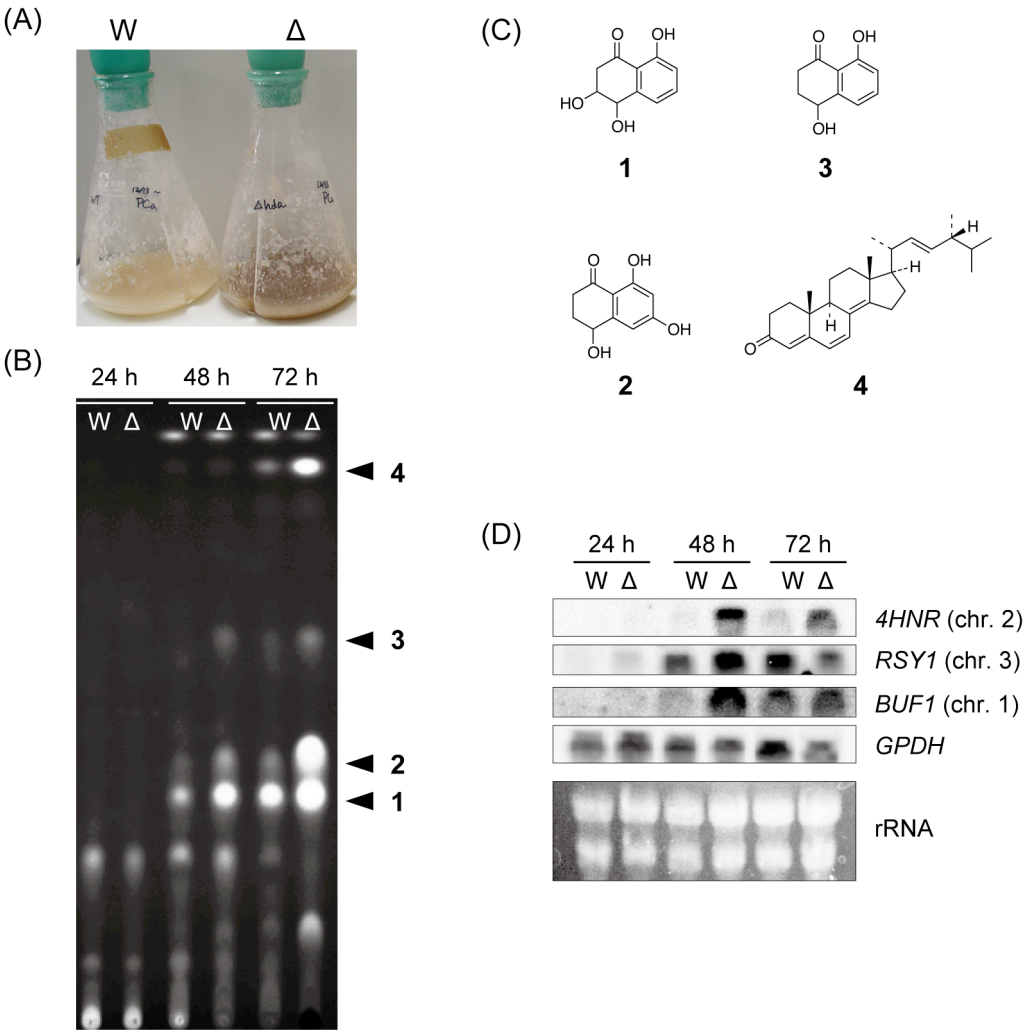

Figure 1 Effect of *MoHda1* disruption on the production of natural metabolites. (A) Melanization of *M. oryzae* wild-type (W) and Δ*Mohda1* (Δ) strains. Fungal strains were cultured in liquid YGPCa medium for 72 h at 28°C. (B) TLC of ethyl acetate extracts. The fluorescence was recorded under UV light (312 nm). (C) Structure of metabolites (**1**–**4**) that were increased in the Δ*Mohda1* mutant. Known shunt metabolites in the DHN melanin (**1**–**3**) and ergosterol (**4**) pathways were identified. (D) Northern blot analysis of melanin biosynthesis genes. The northern blot was hybridized with probes against melanin and glyceraldehyde-3-phosphate dehydrogenase (*GPDH*) (MGG_01084) genes. Ethidium bromide staining of rRNA at the bottom shows equal loading of RNA.

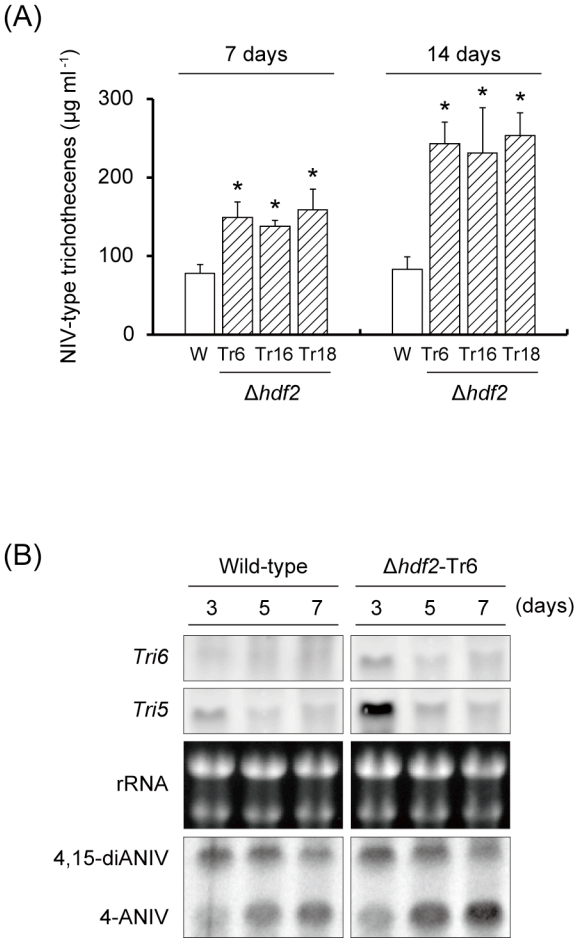

Figure 2 Increased production of trichothecenes after deletion of *HDF2* from *F. asiaticum*. (A) Trichothecene analysis of the wild-type (W) and Δ*hdf2* deletion mutants. After pre-culture on V8 agar for 5 days, three pieces of fresh mycelial plugs were inoculated into 100 ml boiled rice flour liquid medium in a 300 ml Erlenmeyer flask. Total amount of NIV-type trichothecenes (mean ± SD) is based on results from triplicate experiments. Asterisks indicate a significant difference between the wild-type and mutants analyzed by one-way analysis of variance (ANOVA) followed by Dunnett's multiple comparison test; $*P < 0.01$. (B) Northern blot analysis of *Tri* genes and TLC of NIV-type trichothecenes. For isolation of high quality RNA, YS_60 medium was used for trichothecene production. Expressions of *Tri6* and *Tri5* were analyzed at different time points (3, 5, and 7 days after transfer to YS_60 medium)

using RNA isolated from the wild-type and Δ*hdf2*-Tr6 deletion mutant. The type B trichothecenes were visualized under UV light of 254 nm.

Supporting Information

Table S1 Primers used in this study.

Figure S1 Putative shunt pathways and products of DHN melanin and ergosterol.

Figure S2 Complete assignments of ^{1}H and ^{13}C NMR data for compounds **1** - **3**.

Figure S3 Measured electron ionization mass spectrum of **4** (top) and NIST library spectrum of ergosta-4,6,8(14),22-tetraen-3-one (bottom).

Figure S4 Effects of TSA on melanization and metabolite production in *M. oryzae*.

Figure S5 Western blot analysis of nuclei proteins.

Figure S6 Disruption of *HDF2*, the HDA1-type HDAC of *F. asiaticum*.

Figure S7 Deletion of *HDF2*, the HDA1-type HDAC, in *F. graminearum* strain JCM 9873.

Supporting Information

Increased metabolite production by deletion of an HDA1-type histone deacetylase in the phytopathogenic fungi, *Magnaporthe oryzae* (*Pyricularia oryzae*) and *Fusarium asiaticum*

K. Maeda[1,2,3,†], M. Izawa[1,4,†], Y. Nakajima[2,†], Q. Jin[2], T. Hirose[1,3], T. Nakamura[5], H. Koshino[5], K. Kanamaru[2], S. Ohsato[3], T. Kamakura[4] , T. Kobayashi[2], M. Yoshida[1] and M. Kimura[1,2]

[1] Chemical Genetics Laboratory, RIKEN, 2-1 Hirosawa, Wako, Saitama 351-0198, Japan

[2] Department of Biological Mechanisms and Function, Graduate School of Bioagricultural Sciences, Nagoya University, Furo-cho, Chikusa-ku, Nagoya, Aichi 464-8601, Japan

[3] Graduate School of Agriculture, Meiji University, 1-1-1 Higashi-Mita, Tama-ku, Kawasaki, Kanagawa 214-8571, Japan

[4] Faculty of Science and Technology, Tokyo University of Science, 2461 Yamazaki, Noda, Chiba 278-8510, Japan

[5] Molecular Structure Characterization Unit, RIKEN Center for Sustainable Resource Science (CSRS), 2-1 Hirosawa, Wako, Saitama 351-0198, Japan

[†] Joint first authors

Correspondence

Makoto Kimura, Department of Biological Mechanisms and Function, Graduate School of Bioagricultural Sciences, Nagoya University, Furo-cho, Chikusa-ku, Nagoya, Aichi 464-8601, Japan

E-mail: mkimura@agr.nagoya-u.ac.jp

Table S1 Primers used in this study.

primer	primer sequence *	comment
#01	5'- ATGGCTCCCTCCGCAGACAT –3'	primer for preparation of *4HNR* probe
#02	5'- TTAGATACCACCACCGGTCAA –3'	primer for preparation of *4HNR* probe
#03	5'- ACCGCAGTGCTGTGATACCC –3'	primer for preparation of *RSY1* probe
#04	5'- CTCTGGCTCTTTTGATACCT –3'	primer for preparation of *RSY1* probe
#05	5'- ATGCCTGCCGTCACTCAACC –3'	primer for preparation of *BUF1* probe
#06	5'- TTACATGCAAGCACCGCCGT –3'	primer for preparation of *BUF1* probe
#07	5'- TGTGGTATCAACGGTTTCGGTC –3'	primer for preparation of *GPDH* probe
#08	5'- GTCAATGACACGACGGCTGTA –3'	primer for preparation of *GPDH* probe
#09: FgHDA1KO1	5'- TACGCGGCCGCCGCCCAGATGCAGAGATAGTTA –3'	inward primer for construction of pΔFgHda1 disruption vector (*Not*I site created for IPCR)
#10: FgHDA1KO2	5'- ATCGAGCTCGCGCATCCAGATCCTTCATAG –3'	outward primer for construction of pΔFgHda1 disruption vector (*Sac*I site created for vector cloning)
#11: FgHDA1KO3	5'- CATACTAGTAGACGGTGTGTTGGGTTATAGGG –3'	outward primer for construction of pΔFgHda1 disruption vector (*Spe*I site created for vector cloning) and preparation of probe A
#12: FgHDA1KO4	5'- AAAGCGGCCGCTTGAATGGATGAGAATGCGAAAA –3'	inward primer for construction of pΔFgHda1 disruption vector (*Not*I site created for IPCR) and preparation of probe A
#13: dhda1 specific_F	5'- GGTCATTGAATATGCCGACTC –3'	primer for screening of Δ*hdf2* disruption mutant
#14: dhda1 specific_R	5'- TTCCCGGTCTCTGACTACTCT –3'	primer for screening of Δ*hdf2* disruption mutant
#15: check on trpC	5'- TGAATGCTCCGTAACACCCAATA –3'	primer for screening of Δ*hdf2* disruption mutant
#16: check on SacI side	5'- CACTAAAGGGAACAAAAGCTG –3'	primer for screening of Δ*hdf2* disruption mutant
#17: FgHDA-F	5'- GATCCTACCAAACACGCAACACC –3'	primer for preparation of probe B
#18: FgHDA-R	5'- GCAAAGTTGACAACGCCCGTTAT –3'	primer for preparation of probe B
#19: MFTri6-F	5'- GCCTTGCCCCTCTTTGATCGT –3'	primer for preparation of *Tri6* probe
#20: MFTri6-R	5'- TGTTGTCCTTCCTGGTCGTGC –3'	primer for preparation of *Tri6* probe
#21: MFTri5-F	5'- ATCGAGAATTTGCACTATGCT –3'	primer for preparation of *Tri5* probe
#22: MFTri5-R	5'- CTGATCCTTGACCTTTTCATA –3'	primer for preparation of *Tri5* probe

* Restriction enzyme recognition sites created for primers are underlined.

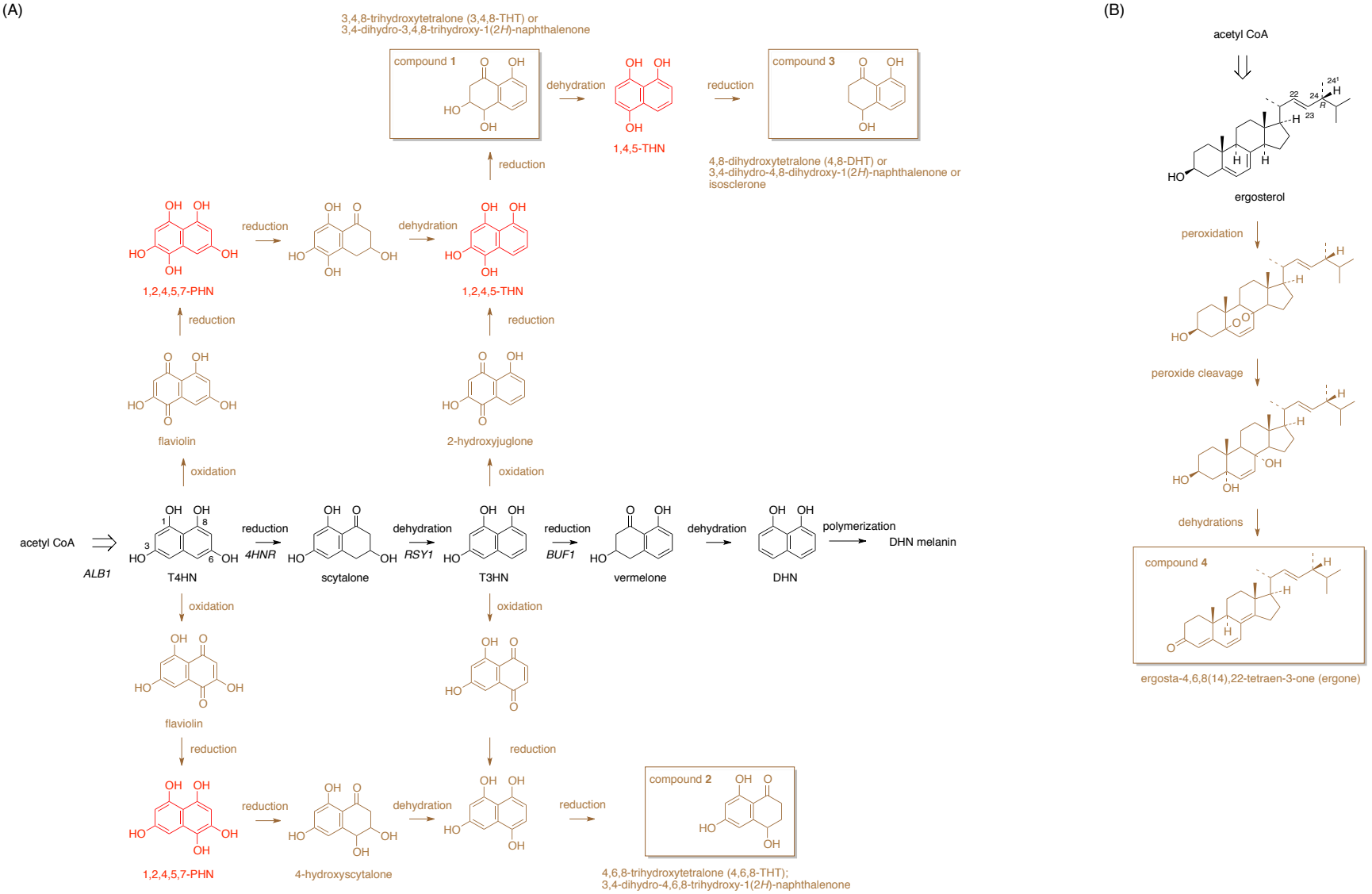
(A)
3,4,8-trihydroxytetralone (3,4,8-THT) or
3,4-dihydro-3,4,8-trihydroxy-1(2H)-naphthalenone
compound 1
dehydration
1,4,5-THN
reduction
compound 3
4,8-dihydroxytetralone (4,8-DHT) or
3,4-dihydro-4,8-dihydroxy-1(2H)-naphthalenone or
isosclerone
reduction
reduction
dehydration
1,2,4,5,7-PHN
1,2,4,5-THN
reduction
reduction
flaviolin
2-hydroxyjuglone
oxidation
oxidation
acetyl CoA
ALB1
reduction
4HNR
dehydration
RSY1
reduction
BUF1
dehydration
polymerization
DHN melanin
T4HN
scytalone
T3HN
vermelone
DHN
oxidation
oxidation
flaviolin
reduction
reduction
1,2,4,5,7-PHN
reduction
4-hydroxyscytalone
dehydration
reduction
compound 2
4,6,8-trihydroxytetralone (4,6,8-THT);
3,4-dihydro-4,6,8-trihydroxy-1(2H)-naphthalenone
(B)
acetyl CoA
ergosterol
peroxidation
peroxide cleavage
dehydrations
compound 4
ergosta-4,6,8(14),22-tetraen-3-one (ergone)

Figure S1 Putative shunt pathways and products of DHN melanin and ergosterol. (A) DHN melanin biosynthetic pathway (black) and related pentaketide shunt pathways (maroon). Structures of melanin shunts (**1**−**3**) that were increased in the Δ*Mohda1* strain are highlighted by shaded boxes. Compounds depicted in red are extremely unstable and have not been isolated. Biosynthetic genes of DHN melanin are indicated by italicized symbols. Abbreviations not mentioned in the main text: 1,2,4,5,7-PHN, 1,2,4,5,7-pentahydroxynaphthalene; 1,2,4,5-THN, 1,2,4,5-tetrahydroxynaphthalene; 1,4,5-THN, 1,4,5- trihydroxynaphthalene (B) Hypothetical ergosterol shunt pathway (maroon). Structure of ergosterol shunt (**4**) is highlighted by a shaded box.

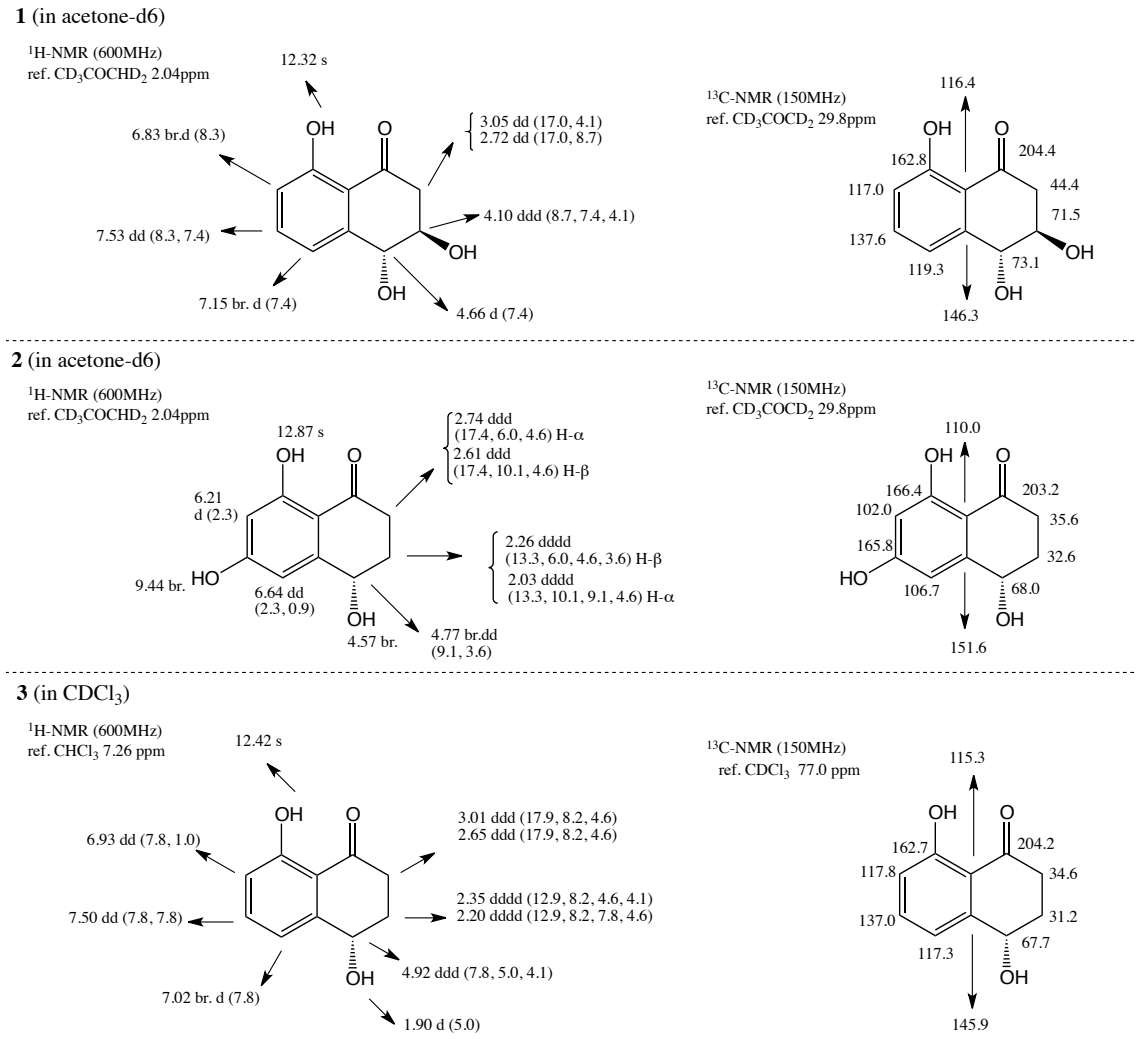

Figure S2 Complete assignments of ^{1}H and ^{13}C NMR data for compounds **1** − **3**. Those assignments were confirmed by analysis of HSQC and HMBC spectra.

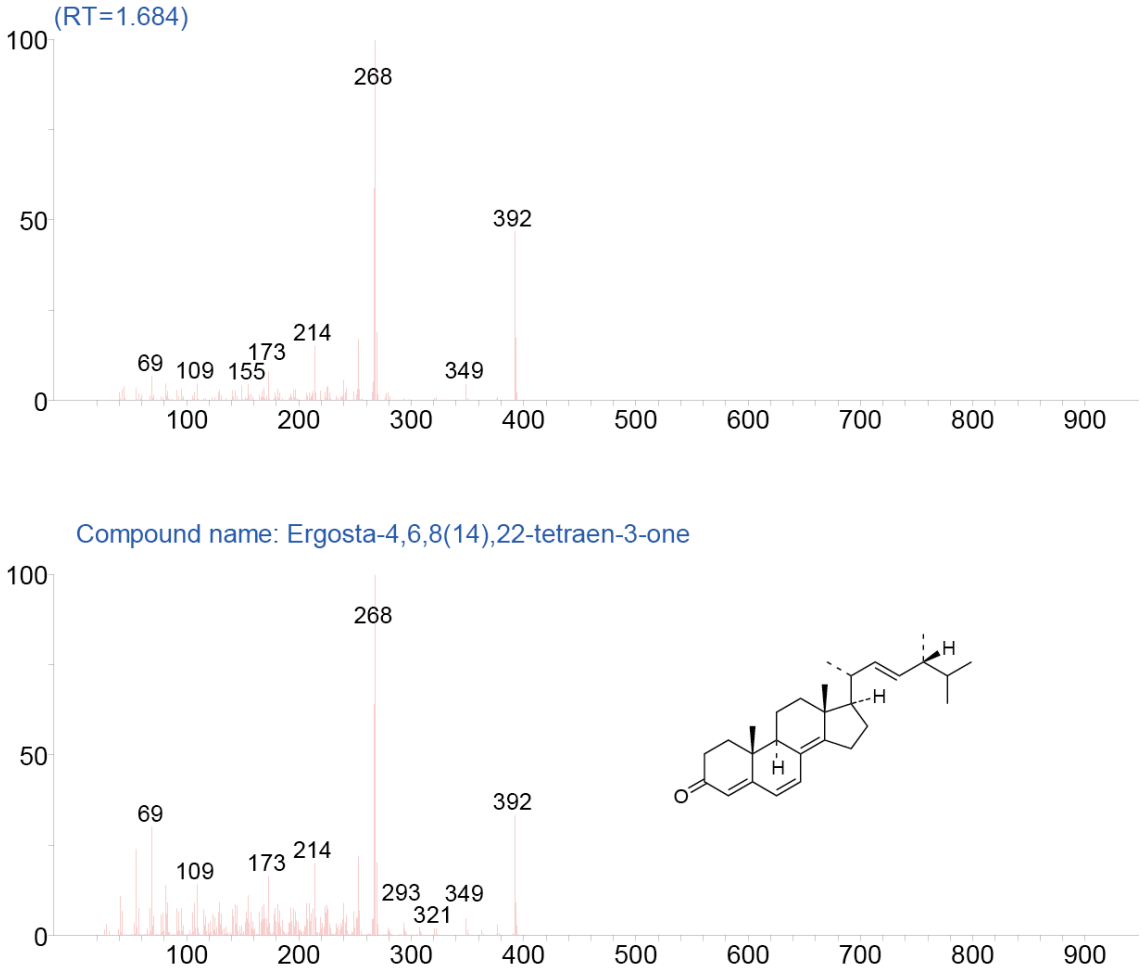

Figure S3 Measured electron ionization mass spectrum of **4** (top) and NIST library spectrum of ergosta-4,6,8(14),22-tetraen-3-one (bottom).

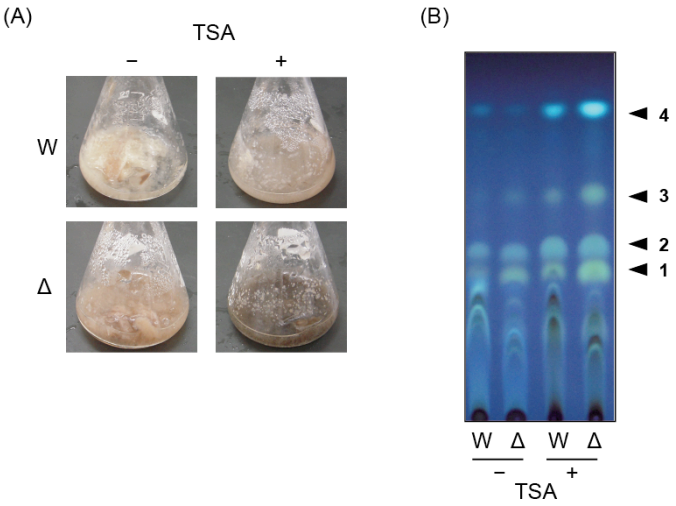

Figure S4 Effects of TSA on melanization and metabolite production in *M. oryzae*. Wild-type (W) and Δ*Mohda1* (Δ) strains were cultured in YGPCa medium with or without TSA (1 μg ml^{-1}). (A) Melanization of fungal strains after 4 days of incubation. TSA and Δ*Mohda1* mutation showed a synergistic effect on melanization. (B) TLC of ethyl acetate extract of wild-type (W) and Δ*Mohda1* (Δ) strains after 4 days incubation in YGPCa medium. The metabolites were visualized by fluorescence at an excitation wavelength of 312 nm.

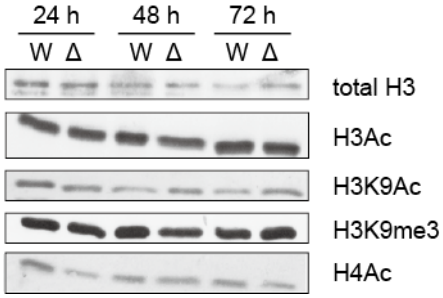

Figure S5 Western blot analysis of nuclei proteins. Global acetylation patterns were monitored using specific anti-histone antibodies. Nuclei were isolated from mycelia as previously described (Palmer *et al*. 2008). For western blot analysis, 15 µg of nuclei proteins was loaded into each lane of a 12.5% SDS-polyacrylamide gel, separated by SDS-PAGE, and transferred to a polyvinylidene difluoride (PVDF) membrane (Bio-Rad Laboratories Inc., Hercules, CA). The PVDF membrane was probed with the following rabbit antibodies: anti-histone H3 (Merck Millipore, #07-690), anti-acetyl-histone H3 (Merck Millipore, #06-599), anti-histone H3 (acetyl K9) (Abcam, Cambridge, UK, ab4441), anti-histone H3 (tri methyl K9) (Abcam, ab8898), and anti-acetyl-histone H4 (Merck Millipore, #06-598). Primary antibodies were detected using an Immun-Star™ AP goat anti-rabbit IgG (H + L) detection kit (Bio-Rad) according to the manufacturer's instructions.

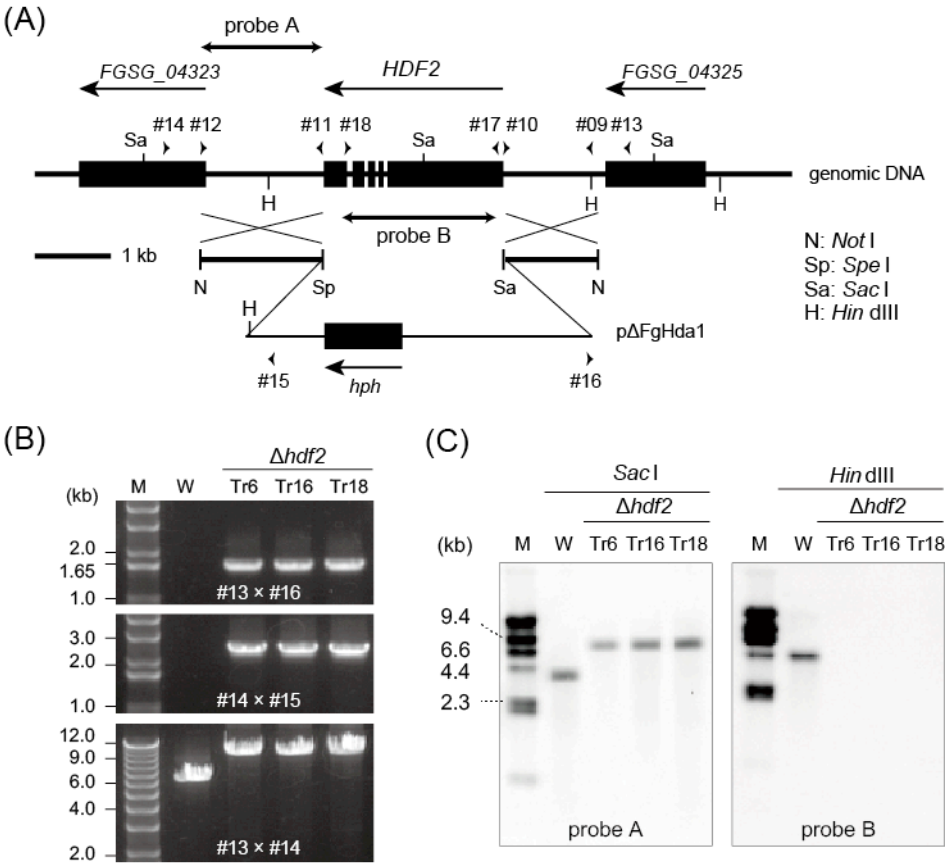

Figure S6 Disruption of *HDF2*, the HDA1-type HDAC of *F. asiaticum*. (A) Schematic depiction of *HDF2* deletion strategy. For construction of pΔFgHda1 by IPCR, primers #09 − #12 (arrowheads; see Table S1 for sequences) and restriction enzymes *Not*I, *Sac*I, and *Spe*I were used. (B) PCR analysis of transformants. Expected band sizes indicative of the *HDF2* disruption (Tr6, Tr16, and Tr18) were obtained by PCR. (C) Southern blot analysis of Δ*hdf2* deletion mutants. Probes A and B were prepared by PCR with primers #11 × #12 and #17 × #18, respectively. Expected band sizes, 3.7 kb from wild-type (W) and 7.7 kb from deletion mutants (Tr6, Tr16, and Tr18), were observed when the *Sac*I blot was hybridized with probe A. Further evidence of successful gene disruption was obtained using probe B, which revealed an expected band size (4.3 kb) on the *Hin*dIII blot of wild-type.

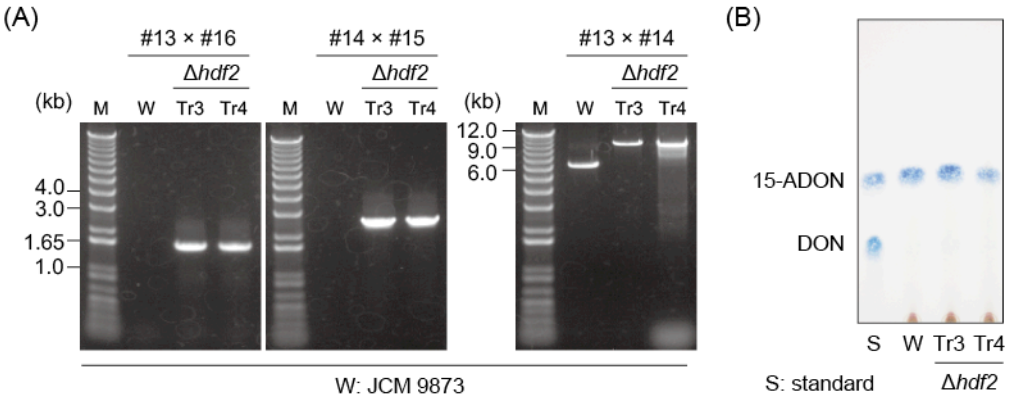

Figure S7 Deletion of *HDF2*, the HDA1-type HDAC, in *F. graminearum* strain JCM 9873. The gene disruption vector pΔFgHda1 was used to delete *HDF2* from JCM 9873. (A) PCR confirmation of the gene deletion. Genomic DNA of wild-type (W) and deletion mutants (Tr3 and Tr4) was used as a template for the PCR assay as described in **Figure S6**. (B) TLC analysis of ethyl acetate extracts of the culture. Wild-type (W) and mutants (Tr3 and Tr4) were cultured at 25^{o}C in 25 ml SYEP medium (6% sucrose, 0.1% yeast extract, 0.1% peptone) in a 100 ml Erlenmeyer flask with gyratory shaking (135 rpm). After 10 days of incubation, metabolites equivalent to 0.5 ml culture supernatant were developed.